Long-term observation of oxygen and isotopes of carbon dioxide in the atmosphere to evaluate the global budget of carbon dioxide (Abstract of the Inter rim Report)

Contact person Tohjima Yasunori
Principal Researcher, Center for Global Environmental Research
National Institute for Environmental Study
Onogawa 16-2,Tsukuba,Ibaraki,305 Japan
Tel:+81-29-850-2485 Fax:+81-29-858-2645
E-mail:tohjima@nies.go.jp

Total Budget for FY2009-FY2013 140,491,000Yen
（**FY2012**;27,494,000Yen）

Key Words Carbon dioxide, Oxygen, Isotope ratio, CO_2 sink, Pacific Ocean

1. Introduction

Carbon Dioxide Information Analysis Center (CDIAC) reported that the global anthropogenic CO_2 emissions from fossil fuel consumptions and cement manufacturing showed an unprecedented increase in the last decade; the global CO_2 emission increased by about 43% between 2000 and 2012. This rapid emission growth has been attributed to the accelerating emissions from the developing countries, especially in China, which achieved remarkable economic growth. Despite the recent decadal exponential increase in the fossil CO_2 emission, the global atmospheric CO_2 growth rate showed a rather stable value of about 2.0 ppm yr^{-1} during the recent decadal period except year-to-year variability of about ±0.5 ppm yr^{-1}. This fact seems to suggest that the land and/or ocean CO_2 uptakes also increased in proportion to the emissions increase. However, several coupled climate-carbon cycle model studies indicated that the global warming would reduce the land and ocean uptakes. In order to predict the future atmospheric CO_2 levels, therefore, it is important to understand the responses of the sink strengths to the suspected climate changes.

Observation of the long-term change in atmospheric O_2 concentration, combined with CO_2 observation, allows us to evaluate the global carbon budgets because of the tightly coupled O_2 and CO_2 exchanges during the land biotic and combustion process. The change in stable carbon isotope of the atmospheric CO_2 can also be used to constrain the global carbon budgets because of the differences in the isotopic fractionation effects between the terrestrial and ocean sink processes. Similarly, carbon-14 content in the atmospheric CO_2 is useful indicator for the influence of the fossil fuel-derived CO_2. Therefore, to better understand the global carbon cycle and its relation to the climate changes, continued, systematic and world-wide observations of the atmospheric O_2 and CO_2 isotopes are desired. However, the observations of the above species are significantly limited in comparison with the observations of the atmospheric CO_2 concentrations because of the difficulty of measuring them.

2. Research Objective

The purpose of this research is to evaluate the accurate terrestrial and oceanic sink fluxes of CO_2, their long-term trend and their interannual variability based on the

atmospheric O_2, CO_2 and CO_2 isotope observations. Additionally, we intend to investigate the relationship between those sink fluxes and climate changes including El Niño and La Niña events. To achieve the extensive and systematic measurements of the atmospheric O_2 and CO_2 isotopes, air samples are collected at two fixed sites (Hateruma (HAT, 24°03′N, 123°48′E) and Ochi-ishi (COI, 43°10′N, 145°30′E)) and commercial cargo ships regularly sailing between Japan and Australia/New Zealand, between Japan and United States, and between Japan and Southeast Asia. We also carry out in-situ measurements of the atmospheric O_2 at HAT and COI, and on board the cargo ship sailing in the western Pacific region. In addition, in order to investigate the influences of the emissions from biomass/fossil fuel burning on our observation, we measure ^{14}C of the atmospheric CO_2 at HAT by using a remote-controlled air sampling system. To improve the CO_2 sink estimations based on the atmospheric CO_2 isotope observations, we also conduct observations of carbon isotopes of dissolved inorganic carbon in the surface seawater. These data would give us the additional information about air-sea O_2 and CO_2 fluxes.

3. Experimental

(1)Air sampling

Figure 1 shows locations where flask samples were collected for the atmospheric O_2, CO_2, and the isotopes measurements and the on-site continuous O_2 measurements were carried out. Air samples were collected in 2~2.5 L Pyrex glass flasks and in 3.3-L stainless steel flasks for the O_2 and the carbon isotope measurements, respectively. We developed and installed a remote-controlled air sampling system at HAT to collect polluted air samples with high CO_2 concentrations (event sampling system), in addition to monthly flask samplings.

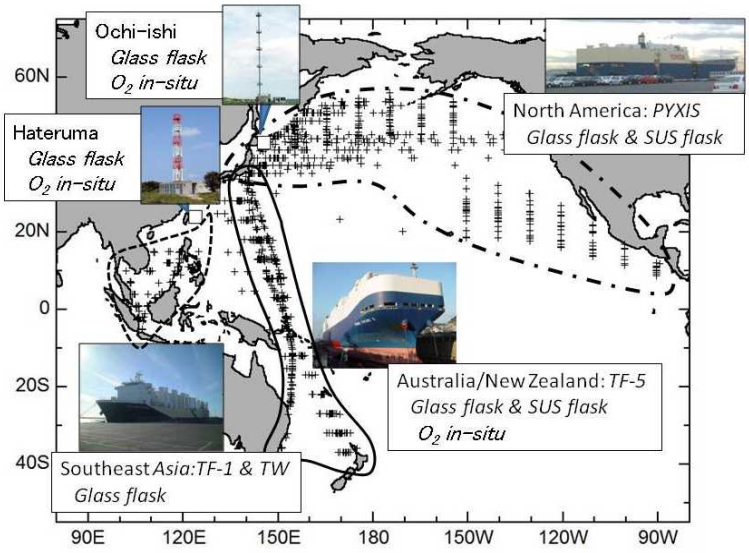

Fig. 1. Positions where flask samples were taken onboard cargo ships (“Trans Future 5”, “Pyxis”, “Fujitrans World” , and “Trans Future 1”) and at two ground-based stations (Hateruma Island (HAT) and Cape Ochi-ishi (COI)).

(2) Analytical methods for air samples

O_2 and CO_2 concentrations of the air samples were measured by a gas chromatograph equipped with a thermal conductivity detector (GC/TCD)[1)] and a nondispersive infrared analyzer (NDIR), respectively. O_2 concentrations are reported as relative deviations of O_2/N_2 ratio from a reference gas[2)]. After the concentration measurements, CO_2 gases in the residual air samples were extracted and analyze the isotope ratios by using an Isotope Ratio-monitoring Mass Spectrometer (MAT 252). In-situ measurements of atmospheric O_2 based on the GC/TCD system were conducted at HAT and COI[3,4)] and onboard the cargo ship (Trans Future 5) sailing between Japan and New-Zealand[5)]. $\Delta^{14}CO_2$ measurements were made using the Compact AMS (Accelerator Mass Spectrometry; NEC 1.5SDH 500kV) performed by Paleo Labo Co., Ltd., Japan. We prepared two whole air reference cylinders to assess a repeatability of $\Delta^{14}C$ measurements.

(3) Analytical methods for water samples

Seawater samples from a pumping line for pCO_2 analyzer are supplied to the measurements of the dissolved components. Dissolved O_2 in seawater was continuously measured by an optical oxygen sensor (OPTODE). In addition, the method of CO_2 co-instantaneously stripping from seawater for $^{13}C/^{12}C$ and $^{14}C/^{12}C$ ratios measurements was developed by improving standard methods.

4. Results

(1) O_2/N_2 measurements and estimation of the global carbon budget

Figure 2 shows a "flying carpet" plot of the latitudinal distribution of the atmospheric O_2/N_2 ratios from the flask samples in the western Pacific over the observation period. The plot clearly shows the secular decreasing trend and the latitudinal differences in the seasonality.

Adopting the APO approach, we estimated the global carbon budgets[2,6]. In this calculation, we use the fossil CO_2 emission estimates from CDIAC database, the global average CO_2 change from NOAA/ESRL observation network, and the ocean outgassing values of 0.5 Pg-C yr^{-1}. Figure 3 shows vector diagram depicting the global carbon budget calculation for the 14-year period (1992 -2013). The oceanic and land biotic sinks for the 14-year period are 2.5±0.7 Pg-C yr^{-1} and 1.5±0.8 Pg-C yr^{-1}, respectively.

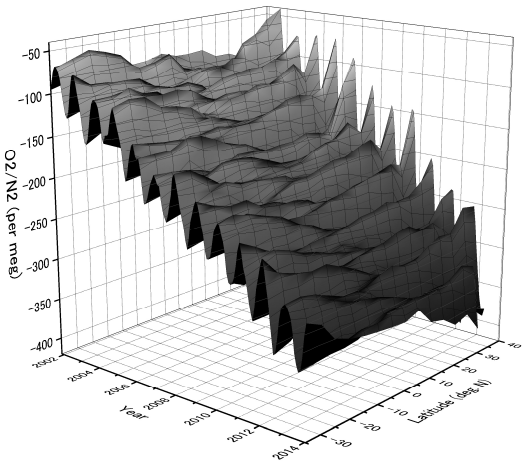

Fig. 2. Temporal change in the latitudinal distribution of the atmospheric O_2/N_2 ratio in the western Pacific region,

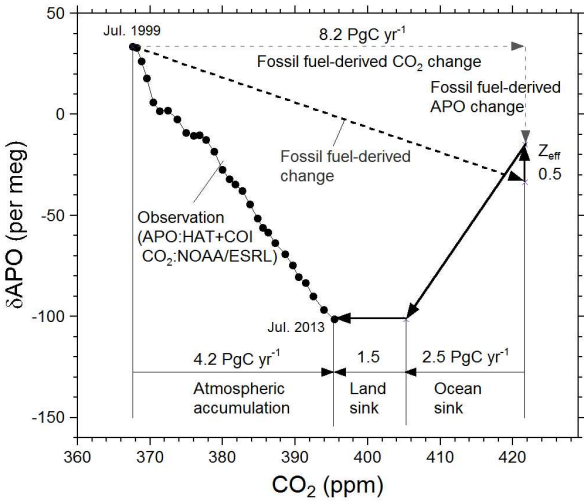

Fig. 3. Vector diagram showing the global carbon budget calculation based on the APO data from HAT and COI and global CO_2 data from NOAA/ESRL.

(2) Variation of CO_2 and carbon isotope ratio in the atmosphere over the Pacific

CO_2 concentration and carbon isotope ratio have been monitored over the Pacific since 1995, and at both Hateruma and Ochi-ishi stations since 1999. Annual change rates in CO_2 concentration and delta ^{13}C value over 17 years were examined in each latitudinal band from 30°S to 60°N to estimate global CO_2 budget in the atmosphere. To obtain global CO_2 budget from isotope analysis, we have to estimate isotope exchange rate between atmosphere and ocean, and the rate between atmosphere and terrestrial biosphere. In this study, we concluded that isotope exchange rate (iso-flux) had to change with time depending carbon cycle rate in each carbon pool, such as ocean and land. We found that some approximation on non-equilibrium term between carbon pools were possible to fit

both ocean and land CO_2 fluxes. Under the certain condition on iso-flux, we estimated the variation of land and ocean CO_2 flux, shown in Fig. 4.

When we compared these results to model results from Global Carbon Project (GCP), we found that trend on our ocean sink estimation was larger than the GCP model calculations. Although our calculation strongly depended on the estimation of iso-flux, the variation pattern of oceanic sink looked reasonable compared to the model calculations. Such differences should be studied more deeply in the future. Concerning on land flux, our results agreed well with average of GCP model estimations, despite that some models showed fairly large sink flux (e.g. VIST model). These comparisons were considered to be very important to evaluate our methodology on long-term flux estimation using isotope analysis.

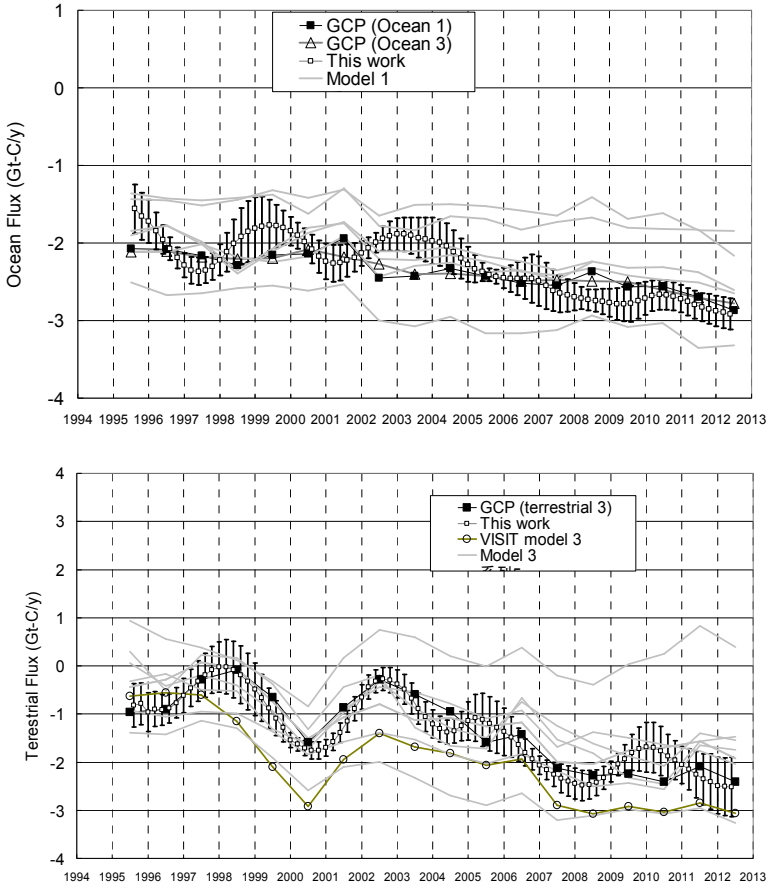

Fig 4. CO_2 budget estimation using carbon isotopic signature

In this study, our isotope observations showed that oceanic and terrestrial sink fluxes became larger gradually, especially after 2004 for the ocean sink and 2006 at terrestrial biosphere.

(3) Radiocarbon measurements at HAT station

Time series of $\Delta^{14}C$ in background air observed at HAT station from 2004 to 2012 indicated that the annual mean $\Delta^{14}C$ values decreased from 58‰ in 2005 to 28‰ in 2012 and the linear trends were -4‰ yr^{-1}. We observed large interannual variability (IAV) in $\Delta^{14}C$ (Fig. 5). The largest anomaly from the linear

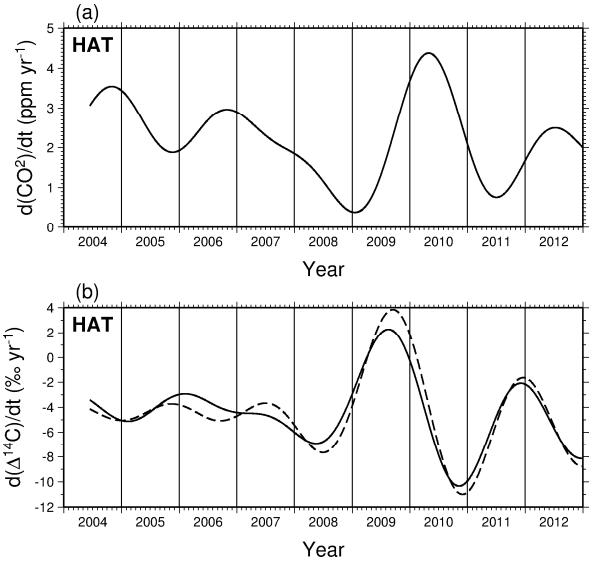

Fig. 5. Time series of growth rate in (a) CO_2 mixing ratio and (b) $\Delta^{14}C$ at HAT. Dashed curves in (b) show the results from the bias-corrected $\Delta^{14}C$.

trends was an increase in 2009 and a decrease in 2010. Comparison of the growth rates in CO_2 and $\Delta^{14}C$ suggests that anomalous decrease in CO_2 in 2009 and increase in CO_2 in 2010 might relate with the inverse changes in $\Delta^{14}C$, although there was a lag of several months to a half year.

We analyzed $\Delta^{14}C$ and $\delta^{13}C$ of 13 high-CO_2 events due to Asian outflow observed at HAT station (Table 1). The CO_2 increases from the background level ($d[CO_2]$) were more than 10 ppm in these events. Fossil fuel-derived CO_2 component (C_{ff}) was calculated as, $C_{ff} = C_{obs}(\Delta^{14}C_{bg}-\Delta^{14}C_{obs})/(\Delta^{14}C_{bg}+1000)$, where C_{obs} is the observed CO_2 mixing ratio (ppm), $\Delta^{14}C_{bg}$ and $\Delta^{14}C_{obs}$ is the background and observed $\Delta^{14}C$ (‰), respectively[7]. We found regional differences in the $C_{ff}/d[CO_2]$ ratio: The $C_{ff}/d[CO_2]$ ratio was lower for the air from China (61% in average) than the other events (81% in average). This suggests larger CO_2 emissions from biosphere over China in winter. We used "Keeling plot" approach to identify the source of the additional CO_2. The results show that the $\delta^{13}C$ value in the air from East China and Yellow Sea is higher than the other events, but with some exceptions. The result is consistent with larger CO_2 emission from cement productions (limestone, $\delta^{13}C$=0‰) in China than in Japan and Korea.

Table 1. Date, origin of air mass estimated using trajectory analysis, $C_{ff}/d[CO_2]$ derived from $\Delta^{14}C$ and equation in the text, and the intercepts of $\delta^{13}C$ Keeling plot for high CO_2 events observed at HAT.

EventID	Date	Air mass from	C_{ff}/dCO_2 (%)	$^{13}C_{source}$ (‰)
1A	2010/03/07-09	Korea	75±6	-29.0
1B	2010/03/09-11	East China	63±0	-24.5
2	2010/04/22-23	Philippine	81±6	-28.1
3	2010/12/13-14	Japan	81±5	-23.9
4	2011/03/01-02	North China	53±6	-24.2
5	2011/04/11-12	Yellow Sea	93±10	-20.3
6	2012/01/19-20	Japan/Yellow Sea	92±7	-22.8
7	2012/02/15-16	Japan/Korea	82±6	-28.6
8	2012/03/07-10	Korea	86±11	-25.8
9	2012/11/11-12	East China	58±5	-23.7
10	2013/01/22-25	East China	73±6	-22.6
11	2013/03/01-02	Yellow Sea/N. China	76±3	-24.1
12	2013/03/13-14	North China	59±13	-26.6
13	2013/04/25-26	Japan/Yellow Sea	67±11	-22.5

(4) $\Delta^{14}C$ analysis of surface water in the western Pacific

Surface $\Delta^{14}C$ in the North Pacific has been monitored using a commercial volunteer observing ship since 2003. Averaged surface $\Delta^{14}C$ in the western subtropical, central subtropical and eastern subtropical regions of the North Pacific for 2003-2008 were 65.8 ± 13.9‰, 65.8 ± 9.6‰ and 46.7 ± 9.4‰, respectively. The long-term $\Delta^{14}C$ decreasing trend after 1970's in subtropical region may have stopped in early 2000's due to a slow decline of atmospheric $\Delta^{14}CO_2$ and having reached equilibrium between atmospheric $\Delta^{14}CO_2$ and the subtropical surface $\Delta^{14}C$.

New method of CO_2 coinstantaneously stripping from only 100mL of seawater for $\delta^{13}C$ and $\Delta^{14}C$ measurements was built up by improvement of each standard stripping method. The method applied to analyze samples taken during the West Pacific (Japan to Australia/ New Zealand) voyages of a commercial volunteer observation ship. The $\delta^{13}C$ of surface water at latitude range from 30°N to 30°S in the West Pacific in July-August of

2010 ranged from +0.35‰ to +1.28‰. The values were high in the northern hemisphere and decreased from equator to southward. We found that the $\delta^{13}C$ of surface water have a good correlation with salinity. On the other hand, the $\Delta^{14}C$ of surface water at the equator, 10°N, 20°N and 30°N during the period of February of 2010 to February of 2011 were shown in Fig. 6. The values ranged from +11‰ to +80‰ and were higher toward high latitude. The $\Delta^{14}C$ at the equator and 10°N decreased in summer season, because surface water of these areas mixed with under layer having low $\Delta^{14}C$ by the equatorial upwelling. These findings of $\delta^{13}C$ and $\Delta^{14}C$ suggest that these parameters are important as tracers for seasonal variation of surface water masses dynamics and air-sea CO_2 gas exchange. Because the $\delta^{13}C$ of surface water is also affected by phytoplankton in euphotic zone, we may be able to explain the effect of phytoplankton on the variation of surface CO_2 concentration.

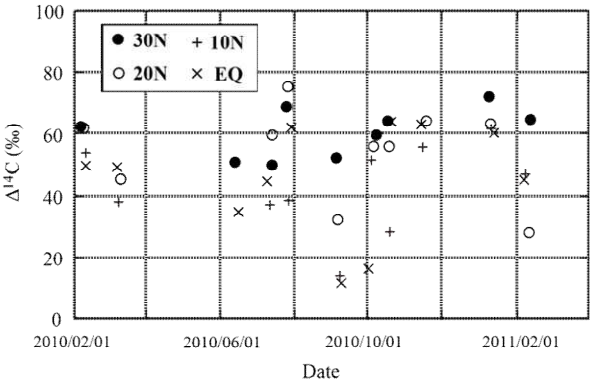

Fig. 6. Seasonal variation of $\Delta^{14}C$ in surface water at the equator, 10°N, 20°N and 30°N in the West Pacific during the period of February of 2010 to February of 2011.

5. Discussion

In order to examine the temporal changes in the individual sink fluxes, we also calculate the carbon budgets for the two periods of 1999-2006 and 2006-2013; the resulted oceanic and land biotic sink fluxes are 2.4 Pg-C yr^{-1} and 0.9 Pg-C yr^{-1}, respectively, for the former period and 2.5 Pg-C yr^{-1} and 2.2 Pg-C yr^{-1}, respectively, for the latter period. Additionally, the carbon budgets estimation based on the ^{13}C measurements also shows significant increases in both uptakes; the oceanic uptake incrases from 2 to 3 Pg-C yr^{-1} while the land uptake increase by about 1.5 Pg-C yr^{-1} during 1995-2013. These results strongly suggest that the enhanced global uptakes, especially land uptake, would compensate the recent accelerated global fossil-derived CO_2 emissions.

The atmospheric $\Delta^{14}C$ measurements at HAT clearly showed the decreasing secular trend and revealed the influence of the fossil fuel-derived CO_2 emissions from the East Asian countries. In addition, we also found the spatio-temproal variations in the $\delta^{13}C$ and $\Delta^{14}C$ values of the dissolved CO_2 in the western and North Pacific. Since these carbon isotopes are closely related to the global carbon cycles, the accumulation of these data would be useful for improving our understanding of the global carbon budgets.

Reference

1) Tohjima, Y. (2000), *J. Geophys. Res.* **105**, 14,575–14,584.
2) Keeling, R. F. and Shertz, S. R. (1992), *Nature* 358, 723–727.
3) Yamagishi, H., Y. Tohjima, H. Mukai, and K. Sasaoka (2008), *Atmos. Chem. Phys.*, 8, 3325-3335.
4) Minejima, C., M. Kubo, Y. Tohjima, H. Yamagishi, Y. Koyama, S. Maksyutov, K. Kita, and H. Mukai (2012) , *Atmos. Chem. Phys*., 12, 1-11, 2012, doi:10.5194/acp-12-1-2012.
5) Yamagishi, H., Y. Tohjima, H. Mukai, Y. Nojiri, C. Miyazaki, and K. Katsumata (2012), *J. Geophys. Res*., 117, D04309, dio:10.1029/2011JD016939.
6) Tohjima, Y., H. Mukai, Y. Nojiri, H. Yamagishi, and T. Machida (2008), *Tellus,* 60B, 213-225, doi:10.1111/j.1600-0889.2007.00334.x.
7) Levin, I., et al. (2003), *Geophys. Res. Lett.*, 30, 2194, doi:10.1029/2003GL018477.